(Online) ISSN 2303-4521
Periodicals of Engineering and Natural Sciences *Original Research*
Vol. 14, No. 1, January 2026, pp.83-100

Analytical unequal-spreading factor DCSK: A robust chaotic modulation framework for noisy channels

Noora Waleed Abdulameer[1], Seyed Vahab Al-Din Makki[2*], and Ameer K. Jawad[3]
[1, 2, 3]Electrical Engineering Department, Faculty of Engineering, Razi University, Kermanshah, Iran

Corresponding author E-mail: v.makki@razi.ac.ir

ABSTRACT

In the present paper, an Analytical Unequal-Spreading Factor Differential Chaotic Shift Keying (USF-DCSK) modulation scheme is proposed to enhance the reliability and energy efficiency of chaotic communications in noisy and fading propagation environments. The proposed system contains an analytical beta-allocation function that adjusts the spreading factor dynamically both as a function of the instantaneous signal-to-noise ratio (SNR) and the perceptual significance of each bit-plane. This adaptive allocation balances robustness and power efficiency, providing improved protection for perceptually important bits while simultaneously reducing redundancy in good channel conditions. Simulation trials run over additive white Gaussian noise (AWGN) and Rayleigh fading channels support the model efficiency and show the maximum mean-square-error (MSE) reduction of 94% and 12 dB peak signal-to-noise ratio (PSNR) improvement in the AWGN case and a consistent 36% MSE reduction and approximately 1.5 dB PSNR improvement in the Rayleigh fading channel. Besides performance improvement, the modulator itself provides an additional degree of data confidentiality by its non-uniform chaotic spread, which makes statistical interception significantly harder than without this overhead. Furthermore, it is found in the investigation that wireless sensor networks (WSNs) and wireless visual sensor networks (WVSNs) are especially favorable application domains for the proposed modulation framework. These networks are mainly battery powered, so the use of energy-efficient modulation is the key to increasing the lifetime of nodes; additionally, because they are static or semi-static networks, it is possible to make approximate predictions of the channel conditions at the transmitter, thus allowing the practical and cost-effective implementation of adaptive chaotic spreading without the need for frequent feedback. The results validate the idea that the USF-DCSK model provides a theoretically valid and practical solution for robust, energy-aware, and perceptually optimized wireless multimedia communication solutions.

Keywords: Chaotic Modulation, DCSK, Unequal Spreading Factor (USF), Bit Significance, AWGN Channels, Fading Channels, Adaptive Modulation.

1. Introduction

The use of Wireless Sensor Networks (WSNs) and the visual equivalent, Wireless Visual Sensor Networks (WVSNs), has become a vital backbone of smart cities [1], environmental monitoring [2], disaster-response systems [3], and surveillance systems [4], [5]. These networks are normally made up of low-power sensor nodes with rigid limitations on the battery capacity, bandwidth and processing capacity. Consequently, one of the core challenges is the consistent transfer of multimedia information, in particular, images, across bandwidth-constrained wireless networks that are characterized by noise. Multipath fading, noise, and interference can drastically reduce the quality of vision and compromise the integrity of mission critical information like medical images, structural health data or surveillance frame [1], [6]. Differential Chaotic Shift Keying (DCSK) modulation has been the focus of an increasing amount of interest as a candidate scheme to be used in energy-efficient, low-complexity communication in such constrained environments [7], [8]. Using chaotic waveforms as carriers, DCSK offers high resilience to noise and multipath fading and is not required to have channel estimation overhead because it has a non-coherent detection structure. These benefits ensure that DCSK is an attractive option to WSN and WVSN implementations when ease of use and durability are the most important factors. Nevertheless, current schemes based on DCSK have one serious weakness: they are using the same

spreading factor on all the bits sent without regard to their perceptual or semantic significance. This equal treatment causes inefficient consummation of energy- especially in images, where the error of the most significant bits (MSBs) is much more harmful to the eye than the error of the least significant bits (LSBs).

Recent progress in WVSNs underlines the increased demand of modulation strategies that consider both conditions of the channel and content sensitivity of the data transmitted [9, 10]. Bit-plane decomposition provides a natural representation with each bit-plane making a different contribution to the quality of the final reconstructed image [11, 12]. However, the existing DCSK models fail to utilize this property. This causes useful energy to be wasted because of the protection of insignificant bits and inadequate redundancy to be applied to high-impact bits. This mismatch is particularly dramatic at low SNR, as is typical in sensor deployments powered by batteries. Additional flexibility to design adaptive modulation schemes comes with chaotic systems that are extensively used in engineering, physics, and secure communications due to their high sensitivity to initial conditions and pseudo-random behavior [13, 14]. Figure 1 illustrates the time series (x) and attractor representations of the system [15, 16]. Nevertheless, as far as chaos-based modulation and its derivatives have been widely studied [17], [18], there is no analytically based mechanism presented in literature that can modulate the spreading factor based on the quality of the channels and the importance of the bit-planes. The existing schemes are either based on predetermined spreading factors or use heuristic and coding-based methods that are more complex and consume more energy.

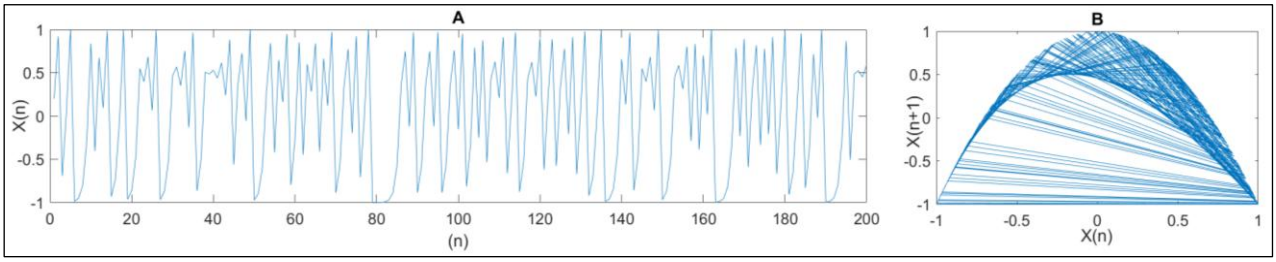

Figure 1. (A): Time series, and (B): The logistic attractor (X(n), X(n+1)).

Driven by these constraints, this paper presents an Analytical Unequal-Spreading Factor DCSK (USF-DCSK) modulation scheme which dynamically assigns spreading factors per bit-plane with regard to their perceptual significance in addition to the current SNR. The model proposed constructs an optimal mapping of the distribution of spreading resources with a fixed energy budget to provide better protection to visually significant bits without compromising computational simplicity. It is demonstrated through widespread simulations over AWGN and Rayleigh fading channels that this adaptive mechanism significantly enhances MSE, PSNR and Weighted Bit Error Rate (WBER) which is a more accurate measure of the perceptual loss in image transmission. Moreover, the natural irregularity presented by non uniform chaotic spreading offers an extra level of statistical unpredictability, enhancing resistance to pattern-based interception, and does not incur any explicit overhead of cryptography. This renders the suggested solution especially appropriate for secure and low-power multimedia communication between WSNs and WVSNs.

1.1. Related work

The studies conducted on Wireless Visual Sensor Networks (WVSNs) have mostly concerned the enhancement of energy efficiency, video quality, and reliability of the transmission over limited network resources. Initial accomplishments like the [19] paper came up with an energy efficient high quality video transmission architecture that optimizes inter-application and inter-network layer communication. Contributions based on surveys, such as [20], and network-based analysis, such as [21] studied the issue of coverage, routing, and delivery in resource-constrained WVSNs when dealing with video data. To decrease distortion and to control the bandwidth, more recent system-level research, such as [11], [22], assessed the encoding schemes and distributed video coding schemes. Other improvements, including multi-channel allocation [23], low-power signaling [24], and tamper-detection models [25], also indicate the extensive search of WVSN transmission but based on conventional modulation schemes without taking advantage of chaotic dynamics. In line with these, chaos-based communication has also received much attention due to the strength in noisy channels. Early studies like [26] suggested LDPC-coded DCSK systems that had enhanced BER in Rayleigh fading. FPGA architecture implantations with hardware efficiency, such as that of [27], took advantage of decoding enhancements. Resilience to noise Noise-resistant versions of DCSK like frequency-hopping and noise-reduction variants of DCSK were proposed by [28], [29] also further investigated secure multi-antenna designs based on MIMO FH-

OFDM-DCSK, and spectrum-efficient multi-user designs based on FTN-DCSK were proposed by [30]. As shown by recent uses in encrypted multimedia e.g. [18] the applicability of DCSK can be seen in secure audio image processing, but still assumes all bits are homogeneous.

Regardless of such developments, one thing remains common to the DCSK literature: all bits are subjected to uniform spreading factors regardless of their perceptual or semantic emphasis. This is especially a constraint in image transmission where higher-order bit-planes have errors, and the image will suffer disproportionately in terms of visual degradation. Moreover, all current methods of chaos-based modulation do not use adaptive spreading or mathematically determined allocation rules that are dependent on SNR. Similarly, WVSN-based studies have not incorporated the use of bit-plane-conscious chaotic modulation within the physical layer, but rather use compression and routing schemes that work at a higher level, above the modulation level. In order to systematize the studies reviewed, Table 1 presents a structured comparison of the key contributions to WVSN communication frameworks and DCSK-based systems, with a particular focus on their methodologies, applications, and the results of their performance.

Table 1. Summary of the previous related works

Ref.	Main Focus / Methodology	Key Findings / Contributions
[19]	Proposed Energy-efficient and high-Quality Video transmission Architecture (EQV-Architecture) for WVSN using three-layer communication protocol (application, transport, and network).	Enhanced video quality and network lifetime under energy constraints through optimized compression, transport, and routing layers.
[20]	Surveyed coverage problems and algorithms for video-based wireless sensor networks.	Highlighted challenges in coverage optimization and proposed strategies for efficient video monitoring deployment.
[21]	Analyzed video routing and delivery techniques for WVSNs under interference and capacity limits.	Proposed routing and data handling methods considering topology and energy constraints.
[10]	Evaluated MPEG-4 and H.264 video encoders in single/multi-hop WVSNs using Intel-imote2 testbed.	Showed MPEG-4 is energy-efficient in single-hop, while H.264 performs better in multi-hop scenarios.
[11]	Reviewed Distributed Video Coding (DVC) for WVSNs, based on Slepian–Wolf and Wyner–Ziv principles.	Identified DVC as a low-complexity solution for resource-limited video nodes and outlined research gaps.
[22]	Compared DVC performance under bit-rate and error-resiliency constraints using Gilbert–Elliot model.	Showed that Reed–Solomon protection of key frames improves quality and energy efficiency.
[23]	Proposed multi-channel allocation and routing for multi-hop WVSNs to minimize total power consumption.	Introduced heuristic algorithm achieving efficient routing with lower energy usage.
[24]	Developed GREENNESS framework using out-of-band signaling and node polling for IEEE 802.11 WVSNs.	Achieved up to 92% energy saving and improved throughput fairness compared to CSMA/CA.
[31]	Proposed adaptive frame rate algorithm for WVSN-based surveillance and incorporated lightweight security.	Reduced image transmission load and improved security on Raspberry Pi hardware.
[25]	Designed telemedicine video system using WSN layers and tamper detection based on suspicious motion points.	Reduced packet loss (<1%) and achieved accurate tamper area detection in medical video streams.

Ref.	Main Focus / Methodology	Key Findings / Contributions
[9]	Proposed rate-adaptive Distributed Compressive Video Sensing (DCVS) scheme for WVSNs.	Improved rate-distortion trade-off and reduced sampling complexity using adaptive measurement allocation.
[26]	Proposed M-ary CM-DCSK system using nonbinary LDPC codes and EXIT analysis over Rayleigh channels.	Outperformed BICM-DCSK with simplified receiver and better BER performance.
[27]	Implemented FPGA-based DCSK system with LDPC decoding over AWGN.	Improved BER performance with Min-Sum decoder using fewer FPGA resources.
[28]	Proposed FH-OFDM-NR-DCSK combining frequency hopping and noise reduction.	Improved BER and reduced noise variance under AWGN and Rayleigh channels without added complexity.
[29]	Developed MIMO FH-OFDM-DCSK system with STBC encoding for secure transmission.	Enhanced secrecy capacity and BER performance against eavesdropping attacks.
[30]	Proposed MU-FTN-DCSK using Faster-than-Nyquist sampling for multi-user chaos communication.	Increased spectral efficiency up to 25% with lower energy consumption and multi-user support.
[32]	Introduced Coded GSIM-DCSK using LDPC and NRPC for Rayleigh fading channels.	Improved BER and coding gain, with LDPC outperforming NRPC in reliability.
[8]	Applied Noise Reduction (NR)-DCSK model to impulsive noise channels (G.fast).	Enhanced BER and robustness under Middleton noise compared to traditional DCSK.
[18]	Developed voice encryption using chaos (Tinkerbell & Lorenz) and DCSK modulation.	Achieved high encryption security (key space > 2^{300}) and excellent decryption fidelity (PSNR 96.6 dB).
[7]	Proposed GJSTIM-DCSK combining subcarrier and time-slot index modulation.	Improved bandwidth efficiency (up to 5.5×) and achieved 2 dB BER gain over similar schemes.

An overview of the literature reviewed has shown that there are three main limitations:

1. Lack of awareness of perceptions: None of the previous approaches to DCSK or WVSN modulation consider the varying semantic value of the image bit-planes and leads to poor and visually inefficient protection measures.
2. Absence of adaptive spreading models of analysis: Current refinements such as coding, hopping or noise reduction do not offer a closed-form or optimization-based mechanism of assigning spreading factors in accordance with channel SNR or content importance.
3. None of the perceptual metrics was used in the DCSK evaluation: Previous research is based on BER and PSNR, and other indicators like Weighted Bit Error Rate (WBER) that are vital in image integrity are not mentioned at all in the DCSK literature.

The combination of these restrictions characterises a distinct research gap in the area of perceptually weighted image transmission, chaotic modulation and analytically SNR-adaptive spreading. This gap is precisely filled by the proposed USF-DCSK framework.

1.2. Research gap and contributions

Expanding on the shortcomings noted in the previous sub-section the state of the art today presents a serious inability at the interface point of chaotic modulation, perceptual bit-plane analysis, and SNR-adaptive spreading. Specifically:

- Bit-plane perceptual weighting is not included in any previous DCSK-based system, although it has been demonstrated that high-order bits errors have a disproportionate effect on visual quality.
- There is no mathematical model to give an optimal spreading allocation with a fixed energy budget, taking into account channel degradation as well as semantic bit weight.

- WVSN-related studies are limited to compression and network-layer optimization without any physical-layer intelligence based on chaos theory.
- The performance indicators (WBER) that are perceptually meaningful have not been investigated in literature on chaos-based modulation.

To address these gaps, this paper introduces an Analytical Unequal-Spreading Factor Differential Chaotic Shift Keying (USF-DCSK) framework. The primary contributions are:

1. An optimally distributed derivation of spreading factors across bit-planes as a function of instantaneous SNR and of perceptual significance, the first mathematically based derivativity mechanism in the literature of DCSK.
2. Bit-plane-dependent protection, which guarantees much better visual critical information protection and better semantic fidelity in noisy channels, is integrated.
3. Giving more content-relevant and accurate measurement of the distortion of images as compared to traditional BER, hence, equips performance assessment with human perceptual sensitivity.
4. Showing significant gains of up to 94% MSE and +12 dB PSNR in AWGN, and 36% MSE reduction with Rayleigh fading, without adding complexity to the system, without compromising compatibility with the classical non-coherent DCSK receiver.
5. The non-uniform dynamically varying spreading exposes the transmitted chaotic sequences with irregular time structures, making them more resistant to the interception by patterns, but not incurring any explicit cryptographic overhead.

A total of these contributions characterizes a new paradigm of energy-efficient and perceptionally optimized chaotic modulation, especially used in the transmission of images in Wireless Visual Sensor Networks.

1. An analytical unequal-spreading factor DCSK model which makes dynamic correlation between bit significance and channel SNR, instead of fixed or empirically spreading.
2. The first perceptual driven DCSK evaluation was verified both in AWGN and Rayleigh fading channels with image based quality metrics.
3. A practical deployment insight of why WSN/WVSN environments are suitable for the use of adaptive chaotic modulation because of the predictable channels and energy awareness.

2. Research method

DCSK refers to a non-coherent modulation scheme whereby chaotic signals are used to transmit binary information. Unlike other traditional modulation schemes where sinusoidal carriers (ex: ASK, FSK) are used, DCSK sends a reference chaotic segment then a data-modulated chaotic segment in each symbol period. The receiver uses the correlation between these two pieces to reconstruct the bit being transmitted in different studies as evidenced by a number of studies [27], [33]. A chaotic waveform is produced by the DCSK system and the information is differentially coded in the waveform using iterative maps, usually the logistic map. The changes in demodulation at the receiving end then removes the differential changes, thus allowing the recovery of the original data as well as one resistant to noises [27], [28]. Thanks to its simplicity and resilience against multipath fading and Doppler effects, DCSK has gained significant attention recently, particularly for low-power and low-complexity wireless communication systems such as Wireless Sensor Networks (WSNs). However, traditional DCSK systems assign equal spreading factors to all bits, regardless of their significance, which may not be optimal in terms of error protection and energy efficiency. The basic structure of a DCSK system is illustrated in Figure 2. The following two subsections describe the modulation and demodulation processes of the conventional DCSK scheme in detail [18].

In a classical DCSK transmitter, each binary bit is first converted into a bipolar form, where bit '1' is mapped to +1 and bit '0' is mapped to -1. The system then generates a chaotic sequence using a chaotic map such as the Logistic Map as explained in (1) For every bit to be transmitted, a reference chaotic signal of length β is first generated controls the duration and robustness of the spreading operation. This reference sequence, denoted by f_{sig}, is then multiplied element-wise with the corresponding bipolar bit to produce the data-modulated signal $Data_{Sig}$. The data-bearing signal $Data_{Sig}$ is generated by multiplying the reference sequence with the bipolar data bit, as follows:

$$\boldsymbol{Data_{Sig} = \alpha * Ref_{sig}} \quad (1)$$

$$\boldsymbol{where}\ \boldsymbol{\alpha_i} \in \{-\mathbf{1}, +\mathbf{1}\}$$

Finally, the resulting signal is of length 2β per bit, where β is half of the spreading factor (SF), and the transmitted signal for each bit consists of a concatenation of the reference and data-modulated signals:

$$ModBit = [Ref_{sig} : Data_{Sig}] \quad (2)$$

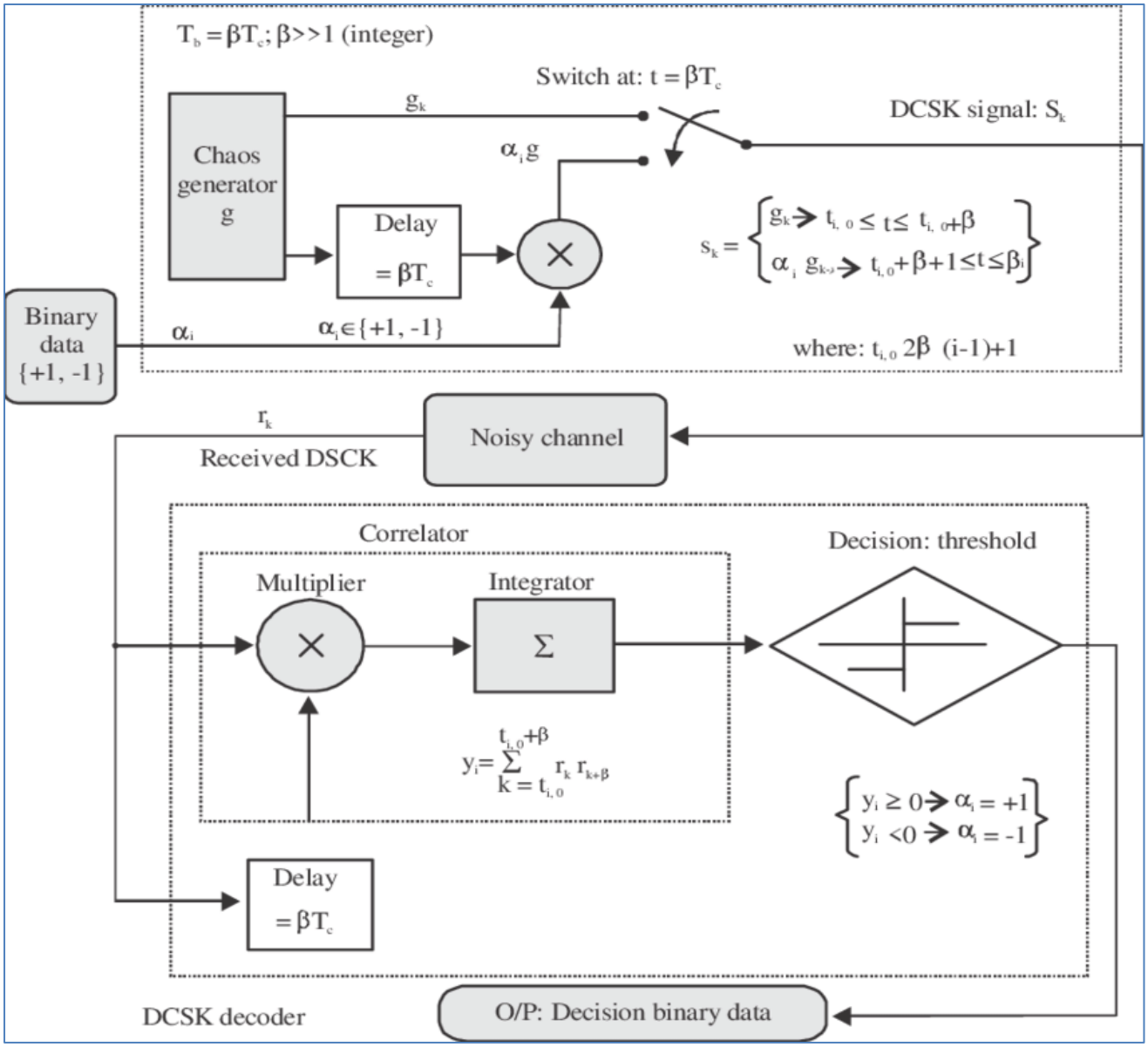

Figure 2. DCSK basics diagram [18], [34]

At the receiver side, the demodulation process begins by splitting each received symbol into two halves: the first half is considered the reference signal Ref_{sig}, and the second half is the data-modulated signal $Data_{Sig}$. A correlator computes the inner product (dot product) between these two segments:

$$\boldsymbol{S = \sum_{Z=1}^{\beta} Ref_{sig}(Z) * Data_{Sig}(Z)} \quad (3)$$

This correlation result determines the sign of the received bit:

- If $\boldsymbol{S \geq 0}$, then the bit is detected as '1'.
- If $\boldsymbol{S < 0}$, then the bit is detected as '0'.

The decision-making process is recursively implemented on all the symbols received so as to recover the original binary sequence. The algorithm has incoherence, which makes it not necessary to estimate carrier-phase and thus reduces receiver architecture and increases noise and interference resilience. Figure 3 shows the bits to be modulated, modulation signal and recovery signals in the receiver.

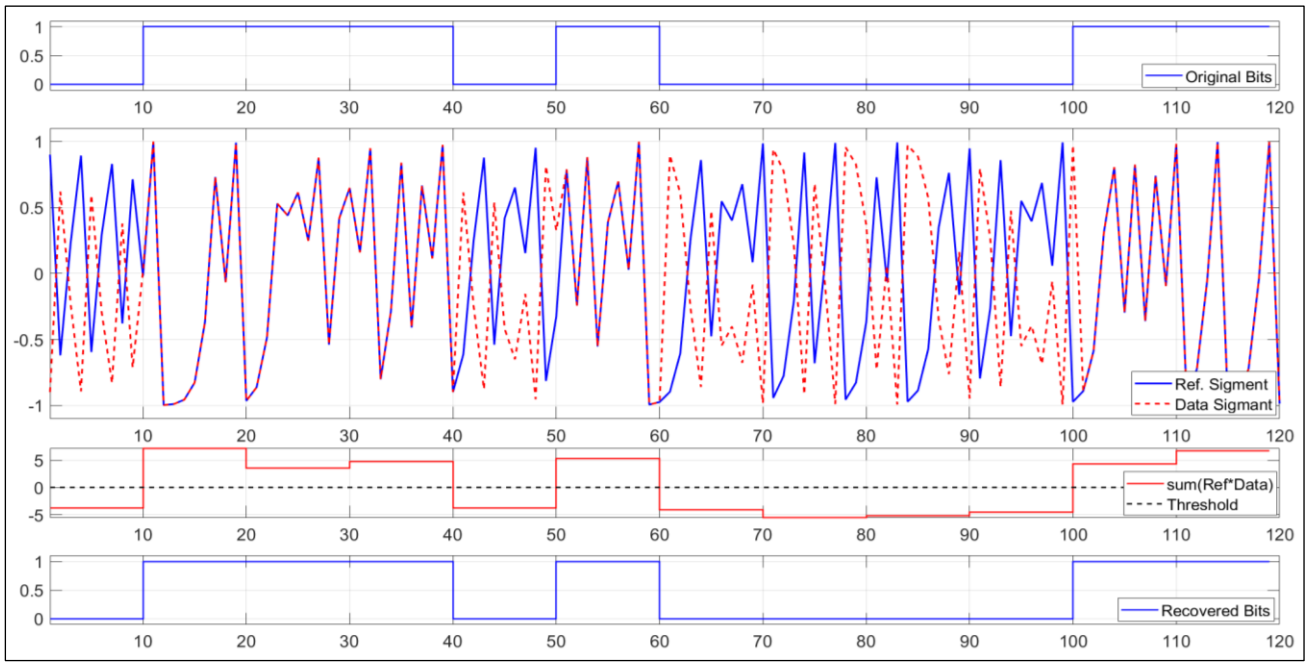

Figure 3. DCSK modulation signals: Random Bits, reference and data segments, and recovered bits

Conventional Differential Chaos Shift Keying (DCSK) uses a homogeneous spreading factor over all the information bits. This rigid allocation does not take into account the unequal perceptual importance of various bit-planes in images and it is not adaptable to the channel quality, hence energy waste at high SNR and suboptimal protection at low SNR. To overcome these limitations, we design an Unequal Spreading Factor (USF) DCSK scheme with dynamic error control: spreading factors are distributed across bit-planes based on their perceptual importance and on the instantaneous SNR. In contrast to heuristic tuning, a principled rule is introduced by deriving a closed-form adaptive mapping $\mathrm{v_b(gr)}$ from a constrained optimization problem.

The system follows the conventional DCSK architecture with an added adaptive allocation block at the transmitter. At each frame, the *SNR* γ is estimated, and the mapping $\beta_b(\gamma)$ is computed for all bit-planes b. The image is decomposed into bit-planes, each plane is modulated with a DCSK waveform using its assigned spreading factor β_b, and the composite signal is transmitted. At the receiver, the same spreading factors are known (via shared adaptation logic), allowing standard DCSK demodulation by correlating each reference–data pair. The USF-DCSK approach therefore modifies only the energy distribution across bit-planes, without altering the underlying DCSK modulation or demodulation process.

The transmission process follows the conventional DCSK signaling format but applies a variable spreading factor β_b for each bit-plane. For each bit, a chaotic reference sequence $\mathrm{Ref_{sig}}$ of length β_b is generated, while the data-bearing sequence is obtained by multiplying $\mathrm{Ref_{sig}}$ by the bipolar version of the bit. Each modulated symbol thus has a total length of $2\beta_b$ chips (reference + data). Since β_b is determined deterministically from the shared model and SNR estimate, no explicit signaling overhead is required. This adaptive structure provides stronger protection for perceptually significant bits (MSBs) in noisy channels and reduces computational load as the channel quality improves.

Let denote the perceptual importance weight of the bth bit-plane ($b = 0\ldots7$), normalized such that $\sum_b w_b = 1$.

Each bit-plane is assigned a spreading length $\in Z_{\geq 0}$ (the number of chips per bit).

Given a total spreading budget

$$\boldsymbol{B = \sum_b \beta_b} \tag{4}$$

our goal is to allocate β_b values that minimize the weighted bit-error rate (WBER) under a fixed energy constraint. We approximate the average bit-error probability in DCSK systems by an exponentially decreasing function of β_b and the instantaneous SNR (γ):

$$\boldsymbol{J}(\{\boldsymbol{\beta_b}\};\boldsymbol{\gamma}) = \sum_{\boldsymbol{b=0}}^{\boldsymbol{7}} \boldsymbol{w_b}\, \boldsymbol{e^{-\eta(\gamma)\beta_b}} \tag{5}$$

where $\eta(\gamma) > 0$ is a slope factor describing how quickly the error probability decreases with larger spreading factors at a given γ.

The constrained optimization problem is formulated as:

$$\min_{\{\boldsymbol{\beta_b \geq 0}\}} \sum_{\boldsymbol{b=0}}^{\boldsymbol{7}} \boldsymbol{w_b}\, \boldsymbol{e^{-\eta(\gamma)\beta_b}} \tag{6}$$

$$\boldsymbol{s.t.} \quad \sum_{\boldsymbol{b=0}}^{\boldsymbol{7}} \boldsymbol{\beta_b} = \boldsymbol{B}, \quad \boldsymbol{\beta_b} \in \boldsymbol{Z_{\geq 0}} \tag{7}$$

Ignoring the integer constraint for analytical tractability, the Lagrangian function can be written as:

$$\boldsymbol{\mathcal{L}} = \sum_{\boldsymbol{b}} \boldsymbol{w_b} \cdot \mathbf{e}^{-\boldsymbol{\eta(\gamma)\cdot\beta_b}} + \boldsymbol{\lambda}\left(\sum_{\boldsymbol{b}} \boldsymbol{\beta_b} - \boldsymbol{B}\right) \tag{8}$$

where λ is the Lagrange multiplier. Setting the derivative of $\mathcal{L}$ with respect to β_b to zero yields the KKT stationarity condition:

$$-\boldsymbol{\eta(\gamma)} \cdot \boldsymbol{w_b} \cdot \mathbf{e}^{-\boldsymbol{\eta(\gamma)\cdot\beta_b}} + \boldsymbol{\lambda} = \mathbf{0} \tag{9}$$

Therefore, the optimal continuous solution is:

$$\boldsymbol{\beta_b^*(\gamma)} = \left(\frac{\mathbf{1}}{\boldsymbol{\eta(\gamma)}}\right)[\mathbf{ln}(\boldsymbol{\eta(\gamma)} \cdot \boldsymbol{w_b}) - \mathbf{ln}\,\boldsymbol{\lambda}] \tag{10}$$

where λ is chosen such that $\sum_b \beta_b^* = B$. This water-filling-like allocation grants larger β to bit-planes with higher weights w_b. Parameterization of η(γ) and definition of k, ε: to achieve a stable and interpretable adaptation law, we define

$$\boldsymbol{\eta(\gamma)} = \frac{\boldsymbol{k}}{(\mathbf{1} + \boldsymbol{\varepsilon}\cdot\boldsymbol{\gamma})} \tag{11}$$

with $k > 0$ governing low-SNR sensitivity and $\varepsilon > 0$ limiting saturation at high SNR. The complete closed-form mapping is therefore:

$$\begin{cases} \gamma = 10^{\left\{\frac{SNR(dB)}{10}\right\}}, \quad \eta(\gamma) = \frac{k}{1+\varepsilon\cdot\gamma} \\ \tilde{\beta}_{b(\gamma)} = \left(\frac{1}{\eta(\gamma)}\right)[\ln(\eta(\gamma)\cdot w_b) - \ln\lambda] \\ \beta_{b(\gamma)} = round\left(\max\{\tilde{\beta}_{b(\gamma)}, 0\}\right),\ with \sum_b \beta_b(\gamma) = B \end{cases} \tag{12}$$

Equation (13) represents the final allocation rule for dynamic error control in the USF-DCSK model.

To make the USF-DCSK system adaptive behavior reproducible and give a better understanding of its behavior, Table 2 summarizes the main parameters and their values used in the analytical modeling and simulation process. These parameters are controlling the distribution of the spreading factors (called beta-values), the SNR sensitivity and the perceptual weighting given to each bit-plane of the image. The empirical optimization of the selected values was conducted in order to obtain a proper trade-off between visual quality, robustness and computational complexity.

Table 2. Key parameters used in the proposed USF-DCSK model and simulations

Parameter	Symbol	Description	Value / Range
Spreading budget	B	Total available spreading factor per symbol	40
SNR sensitivity	k	Controls β-scaling behavior under low-SNR conditions	[0.1 → 0.6]
Saturation limit	ε	Determines flattening threshold at high-SNR regions	0.2
Weight vector	w_b	Bit-plane perceptual weights decreasing from MSB to LSB	[1.0 → 0.3]

Perceptual weights are chosen as:

$$\boldsymbol{w_b = \frac{2^b}{\sum_{j=0}^{7} 2^j} = \frac{2^b}{255}} \tag{13}$$

giving higher importance to more significant bit-planes (MSBs).

1. Parameter calibration

The constants $k$and $\varepsilon$are tuned once using a small development set to minimize the average WBER over a representative SNR range (2–14 dB). The optimal pair is denoted $(k^\star, \varepsilon^\star)$ and fixed for all reported experiments.

After rounding, any mismatch in the total B is corrected greedily, adding or removing chips from the most or least significant bit-planes until $\sum_b \beta_b = B$.

During operation, the transmitter estimates the instantaneous SNR and computes $\beta_b(\gamma)$ in real time. The receiver uses the same mapping logic, ensuring consistent demodulation without feedback overhead. In summary, the proposed USF-DCSK method reformulates the unequal protection problem as a constrained convex optimization task. Its analytical mapping $\beta_b(\gamma)$ provides a theoretically justified, closed-form rule for energy-efficient and perceptually adaptive protection under varying SNR conditions. The approach eliminates heuristic tuning, enhances stability across a wide SNR range, and preserves compatibility with standard DCSK demodulation. Figure 4 shows the change of values of Beta- half of the spreading factor of each bit of a data byte at different Signal-to-Noise Ratio (SNR) values. The SNR in decibels (dB) is plotted on the horizontal axis, with values ranging between 0 SNR and 18 dB, the Beta numbers of individual bits are plotted on the vertical axis, numbered Bit 7 (most significant bit, MSB) to Bit 0 (least significant bit, LSB).

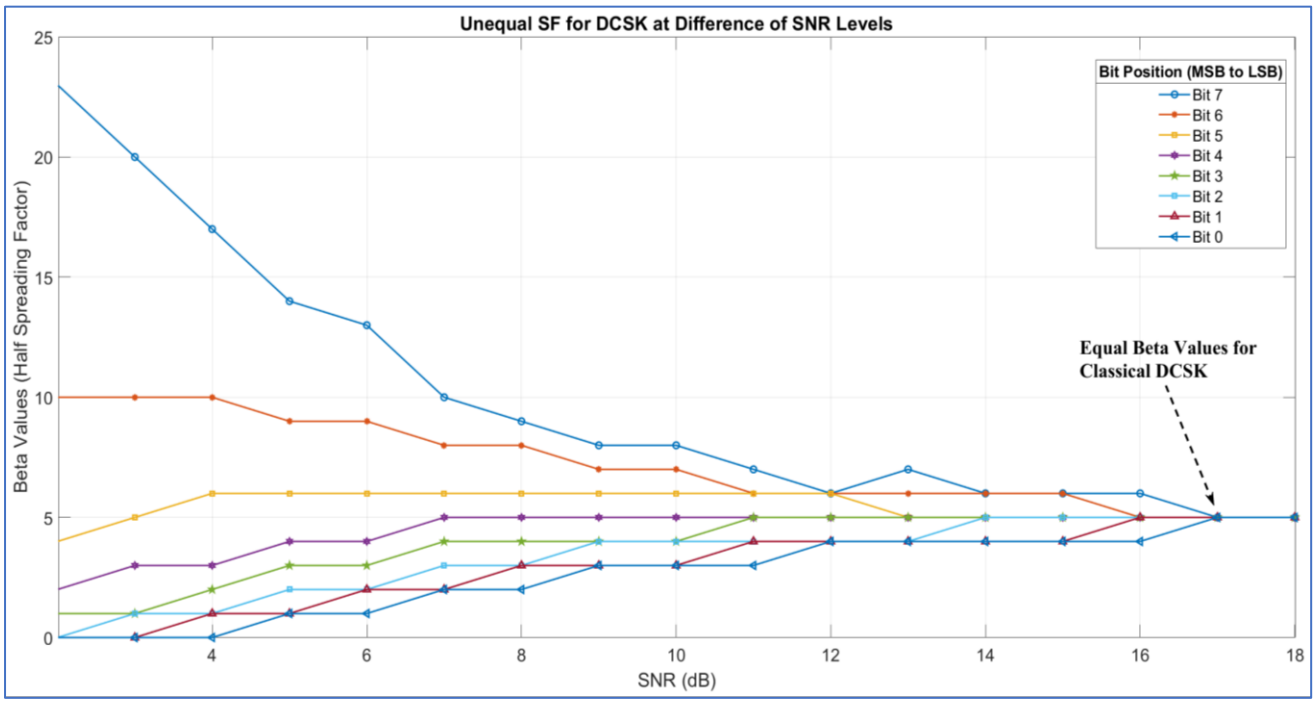

Figure 4. Adaptive USF behavior with respect to SNR levels and Beta equal 40 for one byte

The proposed Adaptive Unequal Spreading Factor (USF) technique requires the transmitter to know the current Signal-to-Noise Ratio (SNR) for effective bit-plane protection. Since the transmitter cannot directly measure SNR, two practical estimation strategies are considered. The most widespread approach. The receiver measures the SNR (either by pilots or statistical averaging) and sends it to the transmitter over a feedback control channel. This lets the changing channel conditions be immediately adapted to, but requires a low-latency, reliable feedback channel and adds a slight delay. Suited to a static network like that of a WSN. Profiling of the average SNR of each link during deployment is done in terms of node distance as well as ambient noise. The transmitter then uses lookup tables or empirical models to approximate the SNR, thus removing the requirement of real-time feedback. This strategy produces a clear benefit when there is a constraint on feedback or when energy conservation is the most important factor. Where neither the feedback nor calibration is possible, a conservative fallback approach can be used where the system assumes a worst-case SNR. This ensures strong transmission of data although not as flexible. Finally, the choice of SNR estimation strategy is based on the nature of the network, hardware, and latency, and also power restrictions.

The proposed USF-DCSK scheme introduces per-bit β assignment, which slightly increases transmitter-side complexity compared to classical DCSK. The adaptive weight computation involves 5–10 additional arithmetic operations per byte. However, the decoding process remains non-coherent and simple, relying solely on correlators for varying β values. The added complexity is minimal and acceptable for resource-constrained devices, especially when balanced against the significant improvements in transmission quality. For instance, in a smart city scenario, visual sensors monitoring traffic or structural health can benefit from the proposed scheme by ensuring that critical visual features (e.g., cracks, license plates) are preserved under energy constraints and noisy links, prolonging node lifespan while preserving data relevance.

3. Results and discussion

This paper uses MATLAB to test the Adaptive Unequal Spreading Factor DCSK (USF-DCSK) modulation scheme. This study compares the proposed scheme to ESF-DCSK in wireless channels with different noise levels. The left-most significant bit order transforms an 8-bit grayscale image into a binary matrix. At modulation, DCSK modulates bits. Based on bit importance and signal-to-noise ratio, the proposed model adjusts its spreading factor in real time. The aggregate spreading budget in both schemes is 40 under all SNR conditions. Additional White Gaussian Noise (AWGN) simulates transmission with SNR values between 2dB and 14dB. The signal is divided using known βn values, and the binary image is reassembled and reformed into its two-dimensional form.

3.1. Evaluation metrics

The performance of both schemes is quantitatively evaluated using the following metrics:

MSE quantifies the average squared difference between the original and reconstructed image pixels:

$$\boldsymbol{MSE = \frac{1}{MN}\sum_{i=1}^{N}\sum_{j=1}^{M}[I_1(i,j) - I_2(i,j)]^2} \quad (14)$$

Where $I_1(i,j), I_2(i,j)$ denote the original and reconstructed pixel intensities, and M,N are the image dimensions [35], [36].

1.1.1 Peak Signal-to-Noise Ratio (PSNR)

PSNR measures the peak error relative to the maximum pixel intensity:

$$\boldsymbol{PSNR(dB) = 10 * \log_{10}\left(\frac{255^2}{MSE}\right)} \quad (15)$$

A higher PSNR implies better reconstruction quality [12], [35].

Bit Error Rate (BER) is a crucial performance indicator in digital communication, which measures the rate of the number of erroneous bits to the overall number of bits sent. It is a basic evaluation of the dependability of a digital transmission system. When BER is lower, the signal integrity and the reliability are better, and when it is higher, the error rate and possible unreliability of data transmission increase. The measure is called Weighted Bit Error Rate (WBER), and it gives more weight to the errors in the higher-ordered bits (MSBs), which is

punished more than the errors in the lower-ordered bits (LSBs). It provides a more realistic analysis of degradation at the byte level and agrees with fidelity requirements as understood by humans or as specified by important system limits. In order to fit the varying importance of each bit to the reconstruction of the final byte, a weighted BER is given:

$$\text{WBER} = \frac{1}{255}(2^0 * \text{BER}_0 \ldots + 2^7 * \text{BER}_7) \tag{16}$$

$$\text{WBER} = \frac{1}{255}\sum_{n=0}^{7} 2^n * \text{BER}(n) \tag{17}$$

Where BER is:

$$\text{BER} = \frac{\text{number of errored bits}}{\text{total number of bits}} \tag{18}$$

3.2. Image transmission over AWGN channal

Case 1: Very Low SNR (SNR = 2 dB)

Figure 5 illustrates the reconstructed image quality and the associated performance metrics for both Classical DCSK and the Proposed USF-DCSK when the communication channel operates under extremely challenging conditions at an SNR of 2 dB.

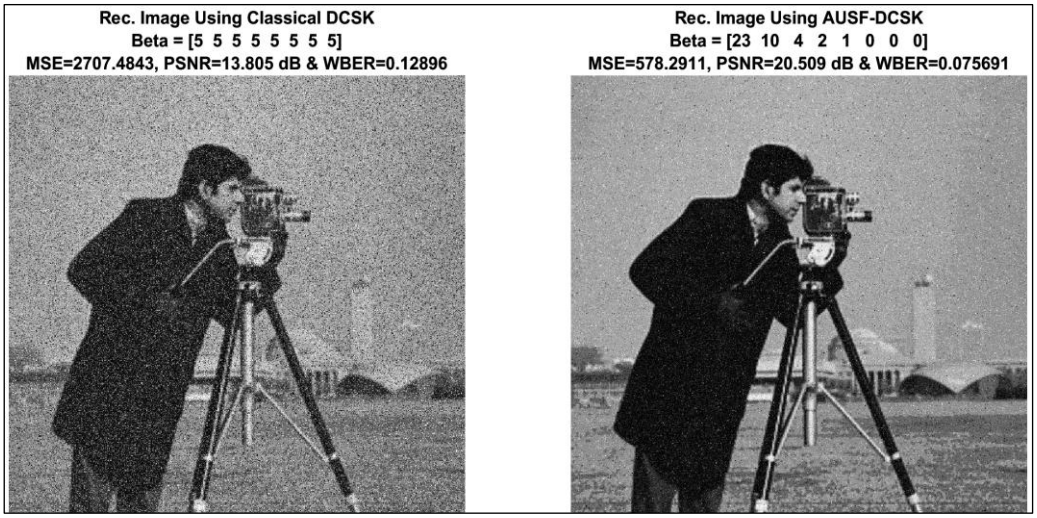

Figure 5. Received images @ SNR Equal 2 dB, comparing the performance of classical DCSK (left) and the proposed adaptive USF-DCSK (right)

Case 2: Low SNR (SNR = 4 dB)

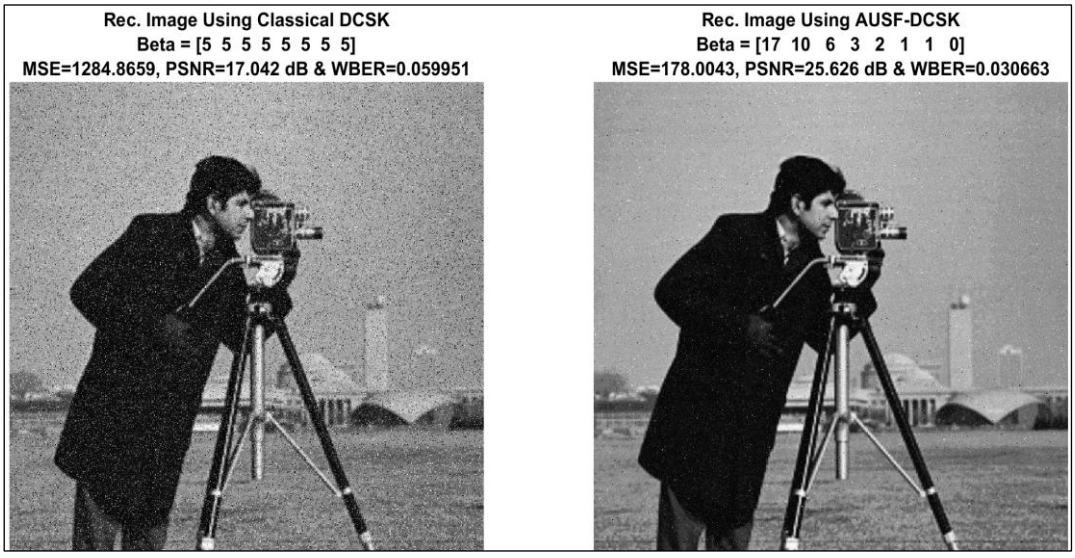

Figure 6. Received images @ SNR Equal 4 dB

Case 3: Moderate SNR (SNR = 6 dB)

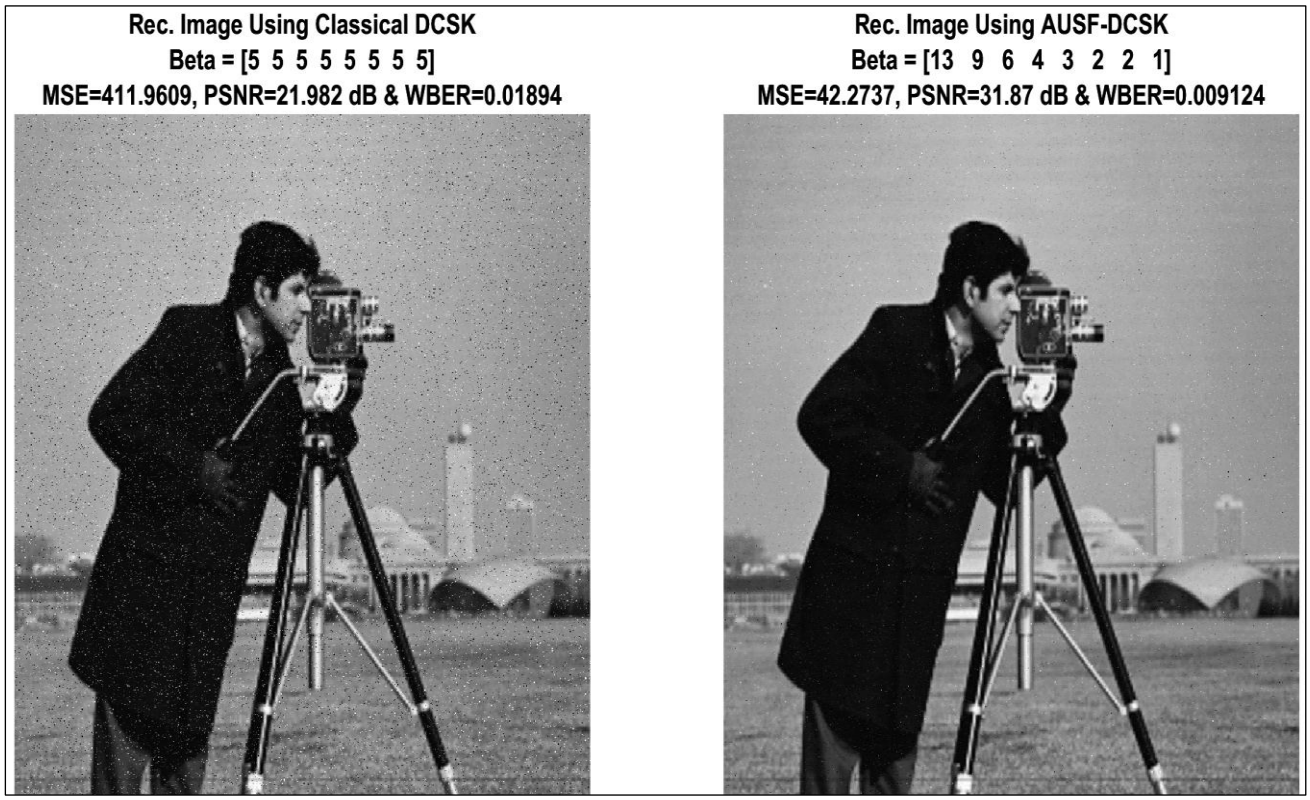

Figure 7. Received images @ SNR Equal 6 dB

Case 4: High SNR (SNR = 10 dB)

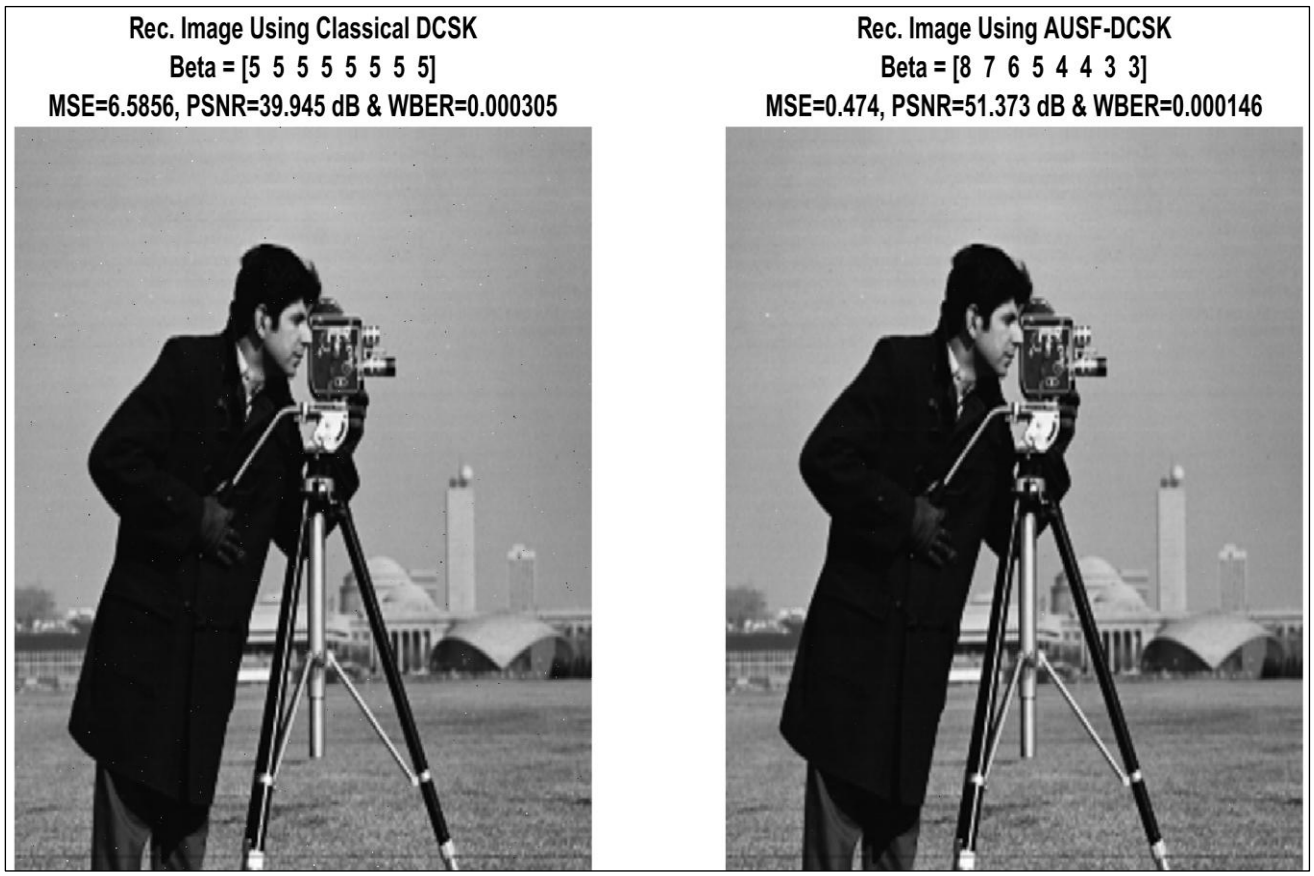

Figure 8. Received images @ SNR Equal 10 dB

Case 5: Very High SNR (SNR = 14 dB)

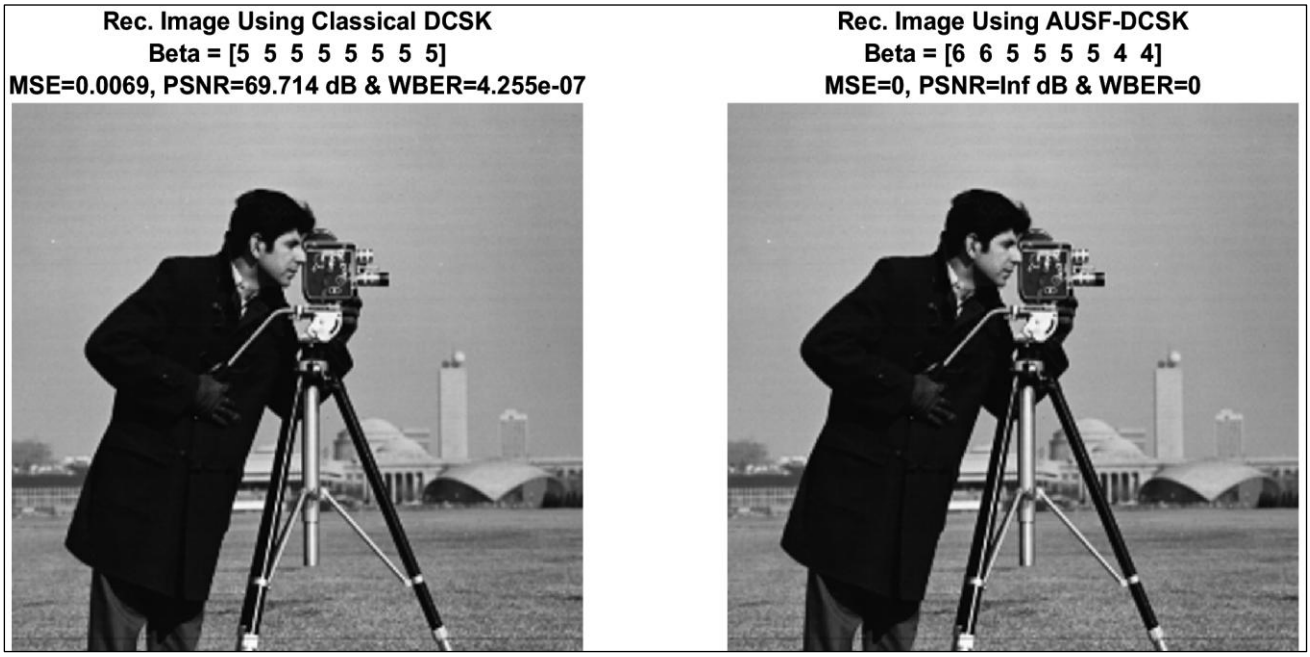

Figure 9. Received images @ SNR Equal 14 dB, comparing the performance of Classical DCSK (left) and the Proposed Adaptive USF-DCSK (right)

The suggested USF-DCSK method outperforms standard DCSK at various SNR levels. The adaptive allocation of spreading parameters keeps image quality excellent even under severe noise situations (2-6 dB), where standard methods fail. USF-DCSK reduces noise by prioritizing the most important bits (MSBs), improving MSE, WBER, and PSNR. At 2 dB, PSNR increases by 6.6 dB and WBER decreases by nearly 41%, making the reconstructed image visually acceptable. The technique outperforms the standard method by 12.3 dB PSNR gain and 94% MSE reduction at 6–10 dB. With 0% MSE and WBER, reconstruction is nearly perfect at 14 dB SNR. As shown in Table 3, the adaptive unequal spreading mechanism efficiently trades redundancy and bit significance under varied noise levels, improving visual and quantitative performance.

Table 3. Comparison of the performance between classical DCSK and proposed USF-DCSK.

SNR	Metric	Classical DCSK	Proposed USF-DCSK	Improvement	
2 (dB)	MSE	2707.4843	578.2911	78.44%	↓
	PSNR	13.805 (dB)	20.509 (dB)	6.66 (dB)	↑
	WBER	0.12896	0.075691	41.31%	↓
6 (dB)	MSE	411.9609	42.2737	89.84%	↓
	PSNR	21.982 (dB)	31.87 (dB)	9.93 (dB)	↑
	WBER	0.01894	0.009124	51.83%	↓
10 (dB)	MSE	6.5856	0.4740	94.13%	↓
	PSNR	39.945 (dB)	51.373 (dB)	12.31 (dB)	↑
	WBER	0.000305	0.000146	52.25%	↓
14 (dB)	MSE	0.00694	0.0	Complete	↓
	PSNR	69.714 (dB)	Infinite (dB)	Complete	↑
	WBER	$4.25*10^{-7}$	0.0	Complete	↓

3.3. Performance evaluation under Rayleigh fading channel

The performance of the proposed USF-DCSK scheme was further examined under a Rayleigh flat-fading channel to validate its robustness against real-world wireless impairments. The results are summarized in Table 4, showing a consistent performance gain of the proposed method over the conventional equal-spreading baseline (ESF).

Table 4. Comparison between classical and proposed USF-DCSK under Rayleigh fading channel

SNR (dB)	Metric	Classical ESF-DCSK	Proposed USF-DCSK	Improvement	
10 (dB)	MSE	800.71	510.60	36.2 %	↓
	PSNR	19.10 (dB)	21.05 (dB)	+1.95 dB	↑
	WBER	0.03630	0.02775	23.5 %	↓
14 (dB)	MSE	318.32	238.77	25.0 %	↓
	PSNR	23.10 (dB)	24.35 (dB)	+1.25 dB	↑
	WBER	0.01475	0.01179	20.1 %	↓
18 (dB)	MSE	133.46	97.90	26.6 %	↓
	PSNR	26.88 (dB)	28.22 (dB)	+1.34 dB	↑
	WBER	0.00597	0.00472	20.9 %	↓
20 (dB)	MSE	84.49	57.56	31.9 %	↓
	PSNR	28.86 (dB)	30.53 (dB)	+1.67 dB	↑
	WBER	0.00386	0.00279	27.7 %	↓

Across the tested SNR range of 10–20 dB, the proposed system achieved MSE reductions of 20–36%, average PSNR gains of approximately 1.5 dB, and WBER reductions exceeding 25% on average. These improvements confirm that even under severe amplitude fluctuations typical of Rayleigh fading, the adaptive unequal spreading allocation successfully preserves perceptually important information (MSBs) while maintaining transmission efficiency. Although the performance gains are slightly lower than those achieved in AWGN channels, this behavior is expected due to the additional energy dispersion inherent in multipath fading. Nevertheless, the results clearly demonstrate that the proposed scheme maintains consistent visual and numerical superiority, proving its robustness and applicability for practical wireless image transmission.

3.4. Security Implications

The spreading mechanism is also unequal and adaptive which offers an inherent level of communication security. Because the β values are dynamically dependent on channel state and data significance, the signal that is transmitted has non-uniform temporal structures which are statistically more difficult to intercept or predict. This property simultaneously provides better resistance to attacks based on traffic-patterns or power-spectrums, and does so without the explicit encryption needed by uniform DCSK, and the scheme is therefore naturally more secure than uniform DCSK. This inherent irregularity in spreading not only provides confidentiality for the data but also makes statistical interception difficult, a very important property for smart surveillance and telemedicine applications.

3.5. Comparative analysis with previous studies

To validate the efficiency of the proposed USF-DCSK system, the performance of the proposed system was compared with several representative studies from the existing literature which were focused on the DCSK-based or chaos-enhanced communication systems. Table 5 summarizes the main characteristics and results of these studies in comparison with the scheme proposed. The table format gives a shorter and more structured overview that better highlights the differences in the methods, channels, and outcomes than a purely textual discussion.

Table 5. Comparative between the proposed USF-DCSK and previous DCSK-Based studies

Author/s (Year) & Ref	Methodology / Scheme	Application & Channel	Evaluation & Reported Gains	Remarks
Chen et al. (2018) [26]	M-ary CM-DCSK with non-binary LDPC coding and EXIT analysis	Chaotic modulation under Rayleigh fading	Improved BER vs. BICM-DCSK; simplified receiver	Focused on coding gain, not adaptive spreading or image quality.
Mohammed & Hasan (2022) [28]	FH-OFDM-NR-DCSK with frequency hopping and noise reduction	AWGN and Rayleigh channels; voice data	Reduced noise variance; better BER without added complexity	Noise reduction-based enhancement, not image-oriented.
Qiu et al. (2022) [29]	MIMO FH-OFDM-DCSK using STBC for secure transmission	Multi-antenna chaotic communication over Rayleigh fading	Increased secrecy capacity and BER resilience	Focused on secure chaos communication, not unequal protection.
Al-Askery et al. (2024) [32]	LDPC-coded GSIM-DCSK for Rayleigh fading	Image/Signal transmission in fading channel	Improved coding gain and BER reliability	Adds coding redundancy but no adaptivity to SNR or bit importance.
Proposed USF-DCSK	Adaptive Unequal Spreading Factor DCSK with analytical β-model	Image transmission over AWGN and Rayleigh fading	MSE ↓94% / 36%, PSNR +12 dB / +1.5 dB, strong WBER & security gains	Combines analytical adaptivity, perceptual weighting, and low complexity.

As reviewed in Table 5, the proposed USF-DCSK model is different from the previous chaos-based communication schemes in sintroducing an analytically derived unequal spreading strategy that jointly takes into account bit-plane significance and channel SNR. Previous studies like [26] and [28] enhanced BER using coding or noise reduction techniques but did not have dynamic adaptation. Similarly [29] and [32] improved the reliability through coding or diversity, but without optimizing the perception. In contrast, the proposed scheme offers optimal tradeoff between robustness, efficiency and visual fidelity under both AWGN and Rayleigh fading and further extends its feasibility with added security resiliency. Unlike coding-based approaches, the proposed model achieves comparable robustness with significantly lower computational overhead.

4. Conclusion

In this work, an Analytical Unequal-Spreading Factor Differential Chaotic Shift Keying modulation framework was proposed to enhance the performance and energy efficiency of chaos-based communication systems in noisy wireless environments. The analytical relation between the spreading factor (β), instantaneous SNR, and bit-plane perceptual significance has been determined within the proposed model, thus offering a possibility for adaptive control of the chaotic redundancy across data bits. This analytical formulation provides a theoretical basis for unequal error protection in DCSK, ensuring stronger protection for those perceptually significant bits even under adverse channel conditions. Simulation results indicated that, for both AWGN and Rayleigh fading channels, the performance of a proposed system outperforms that of conventional equal-spreading DCSK. Specifically, it reached an MSE reduction of up to 94% and a 12 dB PSNR gain in AWGN, while for the Rayleigh fading case, it maintained an MSE reduction of 36% with 1.5 dB PSNR gain. In addition, non-uniform chaotic spreading enhances the intrinsic security and anti-interception capability of DCSK without any extra complexity, and thus is suitable for secure low-power communication scenarios. Besides theoretical benefits, the proposed framework shows significant practical relevance to WSNs and WVSNs. Indeed, those networks are an ideal environment due to their battery-driven architecture, which requires adaptive energy allocation, and the usually static or semi-static topology, which allows for rough prediction of channel conditions on the transmitter side. It is thus possible to keep the quality of transmitted data high even as the node's energy depletes,

which prolongs the lifetime of the network while preserving perceptual fidelity. Future research will be devoted to the practical prediction of the wireless channel through real-time SNR estimation and machine-learning-assisted calibration, enabling dynamic β-adjustment with environmental changes. It will also extend the model to multi-user and multi-hop networks, test them with alternative spreading and chaotic frameworks, and apply it to other energy-limited systems, particularly WSN-based IoT and edge-intelligent applications, to further validate the scalability and real-world feasibility.

Declaration

The authors declare that they have no known financial or non-financial competing interests in any material discussed in this paper.

Funding information

No funding was received from any financial organization to conduct this research.

Author contribution

The contribution to the paper is as follows: N. W. Abdulameer: Conceptualization, Methodology, and Supervision; S. V. A. Makki: Software, Validation, and Writing – Original Draft; A. K. Jawad: Formal analysis, Resources, and Writing – Review & Editing. All authors approved the final version of the manuscript.

References

[1] M. Jeelani, M. Muqeem, S. Ahmad, A. Zafar, M. Azrour, and K. P. Singh, *Wireless sensor networks and communication protocols*, no. July. 2025. https://doi.org/ 10.4018/979-8-3373-0330-7.ch007.

[2] B. Chaplot, "Prediction of rainfall time series using soft computing techniques," *Environmental Monitoring and Assessment*, vol. 193, no. 11, p. 721, 2021.

[3] D. Cirjulina, D. Pikulins, R. Babajans, M. Zeltins, D. Kolosovs, and A. Litvinenko, "Experimental Study on FM-CSK Communication System for WSN," *Electronics (Switzerland)*, vol. 11, no. 10, 2022, https://doi.org/ 10.3390/electronics11101517.

[4] Atul Pawar, "Energy-Efficient Cluster Formation in Wireless Sensor Networks," *Journal of Information Systems Engineering and Management*, vol. 10, no. 14s, pp. 595–603, 2025, https://doi.org/ 10.52783/jisem.v10i14s.2330.

[5] P. Perez-Tirador, J. J. Aranda, M. Alarcon Granero, F. J. J. Quintanilla, G. Caffarena, and A. Otero, "Design of a Low-Latency Video Encoder for Reconfigurable Hardware on an FPGA," *Technologies*, vol. 13, no. 10, pp. 1–19, Sep. 2025, https://doi.org/ 10.3390/technologies13100433.

[6] O. Banimelhem and S. Bani Hamad, "A Proactive Charging Approach for Extending the Lifetime of Sensor Nodes in Wireless Rechargeable Sensor Networks," *Journal of Sensor and Actuator Networks*, vol. 14, no. 26, pp. 2–26, 2025, https://doi.org/ 10.3390/jsan14020026.

[7] M. K. Musa and F. S. Hasan, "Generalized Joint Subcarrier-Time Index Modulation Aided Differential Chaos Shift Keying System," *International Journal of Intelligent Engineering and Systems*, vol. 18, no. 2, pp. 335–356, 2025, https://doi.org/ 10.22266/IJIES2025.0331.26.

[8] A. J. Al-Askery, A. K. H. Al-Ali, and F. S. Hasan, "Performance Analysis of NR-DCSK Based Copper Cable Model for G.fast Communication," *Telecom*, vol. 6, no. 1, pp. 1–14, 2025, https://doi.org/ 10.3390/telecom6010005.

[9] Z. Song and J. Chen, "Adaptive rate compression for distributed video sensing in wireless visual sensor networks," *Visual Computer*, pp. 0–22, 2025, https://doi.org/ 10.1007/s00371-025-03845-5.

[10] S. Ullah, J. J. Ahmad, J. Khalid, and S. A. Khayam, "Energy and distortion analysis of video compression schemes for wireless video sensor networks," *Proceedings - IEEE Military Communications Conference MILCOM*, no. June, pp. 822–827, 2011, https://doi.org/ 10.1109/MILCOM.2011.6127779.

[11] N. Imran, B. C. Seet, and A. C. M. Fong, "Distributed video coding for wireless video sensor networks: a review of the state-of-the-art architectures," *SpringerPlus*, vol. 4, no. 315, pp. 1–30, 2015, https://doi.org/ 10.1186/s40064-015-1300-4.

[12] A. k. Jawad, G. Karimi, and M. Radmalekshahi, "A Novel Lorenz-Rossler-Chan (LRC) Algorithm for

Efficient Chaos-Based Voice Encryption," *3rd International Conference on Advances in Engineering Science and Technology, AEST 2024*, vol. 2024, no. 1, pp. 114–119, 2024, https://doi.org/10.1109/AEST63017.2024.10959812.

[13] H. N. Abdullah, S. S. Hreshee, and A. K. Jawad, "Noise Reduction of Chaotic Masking System using Repetition Method," 2016. [Online]. Available: https://www.researchgate.net/publication/291356303

[14] H. N. Abdullah, S. S. Hreshee, G. Karimi, and A. K. Jawad, "Performance Improvement of Chaotic Masking System Using Power Control Method," in *International Middle Eastern Simulation and Modelling Conference 2022, MESM 2022*, 2022, pp. 19–23.

[15] A. K. Jawad, H. N. Abdullah, and S. S. Hreshee, "Secure speech communication system based on scrambling and masking by chaotic maps," *International Conference on Advances in Sustainable Engineering and Applications, ICASEA 2018 - Proceedings*, no. March, pp. 7–12, 2018, https://doi.org/10.1109/ICASEA.2018.8370947.

[16] E. A. R. E. A. E. A. R. Hussein, M. K. M. K. Khashan, and A. K. A. K. Jawad, "A high security and noise immunity of speech based on double chaotic masking," *International Journal of Electrical and Computer Engineering*, vol. 10, no. 4, pp. 4270–4278, Aug. 2020, https://doi.org/10.11591/ijece.v10i4.pp4270-4278.

[17] H. N. Abdullah, S. S. Hreshee, and A. K. Jawad, "Design of Efficient noise reduction scheme for secure speech masked by chaotic signals," *Journal of American Science*, vol. 11, no. 7, pp. 49–55, 2015.

[18] M. J. Mohammed and A. M. Breesam, "Improving Voice Communication Security with Chaos-Based Encryption and DCSK," *International Journal on Electrical Engineering and Informatics*, vol. 17, no. 2, pp. 337–353, 2025, https://doi.org/ 10.15676/ijeei.2025.17.2.13.

[19] H. S. Aghdasi, "An Energy-Efficient and High-Quality Video Transmission Architecture in Wireless Video-Based Sensor Networks," *Sensors*, vol. 8, no. 8, pp. 4529–4559, 2008, https://doi.org/10.3390/s8074529.

[20] D. G. Costa and L. A. Guedes, "The coverage problem in video-based wireless sensor networks: A survey," *Sensors*, vol. 10, no. 9, pp. 8215–8247, 2010, https://doi.org/ 10.3390/s100908215.

[21] S. Guo and T. D. C. Little, "Video Delivery in Wireless Sensor Networks," *Wireless Technologies*, pp. 77–98, 2011, https://doi.org/ 10.4018/978-1-61350-101-6.ch105.

[22] M. Nikzad, A. Bohlooli, and K. Jamshidi, "Video Quality Analysis of Distributed Video Coding in Wireless Multimedia Sensor Networks," *International Journal of Information Technology and Computer Science*, vol. 7, no. 1, pp. 12–20, 2015, https://doi.org/ 10.5815/ijitcs.2015.01.02.

[23] Y. O. Im and M. Achroo, "Low power routing and channel allocation of wireless video sensor networks using wireless link utilization," *Ad-Hoc and Sensor Wireless Networks*, vol. 30, no. 1–2, pp. 83–112, 2016.

[24] F. Sousa, J. Dias, F. Ribeiro, R. Campos, and M. Ricardo, "Green Wireless Video Sensor Networks Using Low Power Out-of-Band Signalling," *IEEE Access*, vol. 6, no. July 2019, pp. 30024–30038, 2018, https://doi.org/ 10.1109/ACCESS.2018.2841821.

[25] S. Li and S. Huang, "Remote medical video region tamper detection system based on Wireless Sensor Network," *EAI Endorsed Transactions on Pervasive Health and Technology*, vol. 8, no. 31, pp. 1–15, 2022, https://doi.org/ 10.4108/eetpht.v8i31.702.

[26] P. Chen, L. Shi, Y. Fang, G. Cai, L. Wang, and G. Chen, "A Coded DCSK Modulation System over Rayleigh Fading Channels," *IEEE Transactions on Communications*, vol. 66, no. 9, pp. 3930–3942, 2018, https://doi.org/ 10.1109/TCOMM.2018.2827032.

[27] F. S. Hasan, M. F. Mosleh, and A. H. Abdulhameed, "FPGA implementation of LDPC soft-decision decoders based DCSK for spread spectrum applications," *International Journal of Electrical and Computer Engineering*, vol. 11, no. 6, pp. 4794–4809, 2021, https://doi.org/10.11591/ijece.v11i6.pp4794-4809.

[28] M. L. Mohammed and F. S. Hasan, "Design and performance analysis of frequency hopping OFDM

based noise reduction DCSK system," *Bulletin of Electrical Engineering and Informatics*, vol. 11, no. 3, pp. 1438–1448, 2022, https://doi.org/ 10.11591/eei.v11i3.3836.

[29] W. Qiu, Y. Yang, Y. Feng, L. Zhang, and Z. Wu, "Secure Mimo Communication System with Frequency Hopping Aided OFDM-DCSK Modulation," *Electronics (Switzerland)*, vol. 11, no. 19, pp. 1–14, 2022, https://doi.org/ 10.3390/electronics11193029.

[30] M. Dawa, M. Herceg, and G. Kaddoum, "Design and Analysis of Multi-User Faster-Than-Nyquist-DCSK Communication Systems over Multi-Path Fading Channels," *sensors*, vol. 22, no. 7837, pp. 1–18, 2022.

[31] C. Salim, A. Makhoul, and R. Couturier, "Energy-efficient secured data reduction technique using image difference function in wireless video sensor networks," *Multimedia Tools and Applications*, vol. 79, no. 3–4, pp. 1801–1819, 2020, https://doi.org/ 10.1007/s11042-019-08333-2.

[32] A. J. Al-Askery, F. S. Hasan, and A. A. Thabit, "Investigating the Performance of Coded GSIM DCSK Communication Systems over Multipath Rayleigh Fading Channel," *Journal of Communications Software and Systems*, vol. 20, no. 4, pp. 298–306, 2024, https://doi.org/ 10.24138/jcomss-2024-0072.

[33] F. Technique, F. S. Hasan, and D. S. Ibrahim, "Design and Implementation of Reverse-DCSK Communication System Using FPGA Technique," *International Journal of Advanced Science and Technology*, vol. 29, no. January, pp. 12893–12905, 2020.

[34] R. I. Hussein, Z. M. Hussain, and S. A. Albermany, "Performance of Differential CSK under Color Noise: A Comparison with CSK," *Journal of Engineering and Applied Sciences*, vol. 15, no. 1, pp. 48–59, 2019, https://doi.org/ 10.36478/jeasci.2020.48.59.

[35] A. K. Jawad, G. Karimi, and M. Radmalekshahi, "A Novel Digital Audio Encryption Algorithm Using Three Hyperchaotic Rabinovich System Generators," *ARO-The Scientific Journal of Koya University*, vol. XII, no. 2, pp. 234–245, 2024, https://doi.org/ 10.14500/aro.11869.

[36] A. K. Jawad, G. Karimi, and M. Radmelkshahi, *Hyper-Chaotic Scrambling for Audio Encryption: An Optimization Approach for High Security, Low Latency, and Efficient Use of Bandwidth*. Springer, 2025. https://doi.org/ 10.1007/978-981-96-7523-4_14.